

## Observation of spin filtering with a ferromagnetic EuO tunnel barrier

Tiffany S. Santos\* and Jagadeesh S. Moodera

Francis Bitter Magnet Laboratory, Massachusetts Institute of Technology, Cambridge, Massachusetts 02139, USA

(Received 19 April 2004; published 25 June 2004)

Spin polarization ( $P$ ) of the electron tunnel current is observed for a ferromagnetic EuO tunnel barrier between nonferromagnetic electrodes. Spin filtering due to different barrier heights for the spin-up and spin-down electrons gives rise to  $P$ , which was measured using a superconducting Al electrode as the spin detector. A large internal exchange field is exerted by the  $\text{Eu}^{2+}$  ions on the Al quasiparticle density of states, evidenced by enhanced Zeeman splitting even at zero applied field. Using a ferromagnetic barrier to filter spins has potential as a means for injecting a polarized current into semiconductors. Our EuO films show structure, magnetic moment, and Curie temperature matching bulk EuO.

DOI: 10.1103/PhysRevB.69.241203

PACS number(s): 73.40.Rw, 74.50.+r, 72.25.Hg

Efficient injection of highly spin-polarized electrons into a semiconductor is essential to the emergence of spin-based electronics. Much focus is on the development of device structures that inject spin-polarized charge carriers efficiently and maximize spin lifetime during transport as well.<sup>1,2</sup> Many of these studies use a ferromagnet (FM) or a ferromagnetic semiconductor as the source of polarized carriers for injection.<sup>3-7</sup> One such approach is to tunnel spin-polarized electrons from a FM, through an insulating tunnel barrier, into a semiconductor.<sup>8,9</sup> Spin injection via tunneling seems the most promising mechanism since the tunneling process is not affected by the conductivity mismatch between the FM and semiconductor.<sup>10</sup> Measuring polarization of the tunnel current from a FM through an insulating barrier has been extensively practiced with the use of a superconducting aluminum electrode as the spin detector, known as the Meservey-Tedrow technique.<sup>11</sup>

Spin polarization ( $P$ ) of the tunnel current, as seen in the familiar Al/Al<sub>2</sub>O<sub>3</sub>/FM structure, originates from the difference in the spin-up and spin-down electron density of states at the Fermi level in the FM, for the given FM/Al<sub>2</sub>O<sub>3</sub> interface.<sup>11</sup> Instead of using a FM as the source for spin-polarized electrons, this study uses a ferromagnetic tunnel barrier. EuO is a ferromagnetic semiconductor in which exchange splitting of the conduction band ( $\Delta E_{\text{ex}}$ ) creates two different tunnel barrier heights—a lower one for spin-up electrons and a higher one for spin-down electrons. Since the tunnel current is exponentially increased as the barrier height is lowered, EuO effectively filters out the spin-down electrons from an unpolarized current of a nonferromagnetic electrode, thereby resulting in a spin-polarized current.  $\Delta E_{\text{ex}}$  of 0.54 eV in bulk EuO below the Curie temperature ( $T_C = 69$  K) was demonstrated by a redshift of the absorption edge nearly 30 years ago.<sup>12,13</sup> A more recent study<sup>14</sup> utilized spin-resolved x-ray absorption spectroscopy to determine  $\Delta E_{\text{ex}} = 0.6$  eV in EuO films. While creating a source of highly spin-polarized electrons, with a degree of polarization reaching even 100%, continues to be a materials challenge, this study exhibits the spin-filter effect in EuO and thus its potential to generate a highly polarized current of electrons for injection into a semiconductor.

The spin-filter effect has been observed with other europium chalcogenide tunnel barriers EuS<sup>15,16</sup> and EuSe<sup>17</sup> in

the past. Ferromagnetic EuS barriers have shown  $P$  as high as 85% even at zero applied magnetic field, whereas EuSe is an antiferromagnet that becomes ferromagnetic in an applied field, leading to conduction band splitting. Therefore,  $P$  is field dependent for EuSe barriers:  $P=0$  in zero field and increases with applied field, reaching nearly 100% at  $\sim 1$  T. EuS and EuSe have a  $T_C$  of 16.6 K and 4.6 K, respectively. With a higher  $T_C$  and a greater  $\Delta E_{\text{ex}} = 0.6$  eV (compared to  $\Delta E_{\text{ex}} = 0.36$  eV for EuS),<sup>13</sup> EuO holds promise to reach 100% spin filtering at higher temperatures. For a given barrier thickness, because the spin-up (spin-down) tunnel current [ $J_{\uparrow(\downarrow)}$ ] is exponentially dependent upon the corresponding barrier height  $\Phi_{\uparrow(\downarrow)}$ ,  $J_{\uparrow(\downarrow)} \propto \exp[-\Phi_{\uparrow(\downarrow)}^2]$ , a greater  $P = (J_{\uparrow} - J_{\downarrow}) / (J_{\uparrow} + J_{\downarrow})$  can be achieved by EuO.<sup>18</sup> Furthermore, the  $T_C$  of EuO can be raised well above liquid nitrogen temperatures by doping with rare earth metals,<sup>19-21</sup> although doping has been seen to lower  $\Delta E_{\text{ex}}$ .<sup>12</sup>

EuO films were deposited at room temperature via thermal reactive evaporation of an Eu metal source (99.99% pure) in the presence of oxygen. The base pressure of the high-vacuum deposition chamber was  $6 \times 10^{-8}$  Torr, and a small flow of oxygen gas was maintained (pressure at any value up to  $1 \times 10^{-6}$  Torr) during evaporation. The film thickness was measured *in situ* by a quartz crystal monitor, and the deposition rate was  $\sim 0.5$  nm/min. With a heat of formation  $\Delta H_f = -1730$  kJ/mol for Eu<sub>2</sub>O<sub>3</sub> compared to  $\Delta H_f = -608$  kJ/mol for EuO,<sup>22</sup> Eu readily oxidizes to form the more stable compound Eu<sub>2</sub>O<sub>3</sub>. Therefore, careful control of the Eu deposition rate and oxygen flow is crucial to forming the desired EuO phase. In order to confirm the formation of EuO, the structural, optical, and magnetic properties of the film were measured and compared to those of bulk EuO parameters reported in literature. EuO films for x-ray diffraction (XRD), optical absorption, and magnetic property measurement were prepared with a thickness of 7.5–25 nm and with a capping layer of 15 nm Al<sub>2</sub>O<sub>3</sub>, on either quartz or etched  $\langle 100 \rangle$ Si substrates.

To observe the spin-filter effect and measure polarization, tunnel junctions were prepared on glass substrates using shadow masks. The bottom electrode of 4.2 nm Al was deposited onto liquid-nitrogen cooled glass substrates. After the substrate was warmed to room temperature, 1–4.5 nm thick

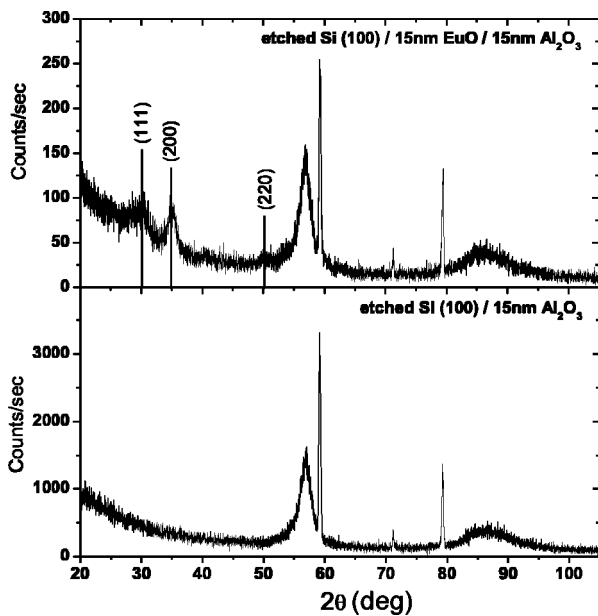


FIG. 1. XRD spectra of 15 nm EuO/15 nm Al<sub>2</sub>O<sub>3</sub> on etched Si(100) (top panel) along with a standard of 15 nm Al<sub>2</sub>O<sub>3</sub> on etched Si(100) (bottom panel), measured in glancing angle mode with  $\theta = 5^\circ$ . XRD lines due to EuO are identified in the top panel.

EuO film was deposited as described earlier. The top electrode was either Y or Al or Ag. All layers were grown by thermal evaporation, and a 5 nm thick Al<sub>2</sub>O<sub>3</sub> capping layer was deposited from an electron-beam source over the entire junction structure. In a given run, 72 junctions were prepared *in situ*, with up to six different thicknesses of EuO barrier. The junction area was  $150 \times 150 \mu\text{m}^2$  for a EuO barrier thickness  $< 3$  nm and  $1.5 \times 1.5 \text{mm}^2$  for thickness  $> 3$  nm, in order to tune the junction resistance to a reasonable value ( $< 50 \text{k}\Omega$ ) for measurement.

X-ray diffraction in glancing angle mode for 15 nm EuO film with 15 nm Al<sub>2</sub>O<sub>3</sub> capping layer on  $\langle 100 \rangle$ Si is shown in Fig. 1. EuO has a face-centered-cubic rocksalt crystal structure. The (111), (200), and (220) peaks of EuO are clearly distinguishable, and match those of EuO powder reference data.<sup>23</sup> The XRD spectra show that the films are polycrystalline. (Growth of epitaxial EuO on Si with a SrO buffer layer has been recently reported.<sup>24</sup>) Optical absorption measured for 15 and 25 nm EuO films grown on quartz closely resembled the absorption spectrum of a EuO crystal, with a band gap of 1.1 eV at room temperature matching the known band gap of bulk EuO.<sup>25</sup>

Magnetic properties of the films were measured using a superconducting quantum interference device (SQUID) magnetometer. Magnetization ( $M$ ) versus applied magnetic field ( $H$ ) taken at 5 K is shown in the inset of Fig. 2 for a 15 nm film (the same film used for XRD) and a 7.5 nm film.  $M(H)$  shows strong ferromagnetic behavior, with a saturation magnetic moment per Eu<sup>2+</sup> ion of  $7.0\mu_B$  and  $7.3\mu_B$  for the 15 and 7.5 nm films, respectively. These values are close to the bulk moment of  $7.45\mu_B$ . Remanent magnetization  $M_r = 5.5\mu_B$  and coercive field  $H_C = 150$  Oe for the 15 nm film, and  $M_r = 6.4\mu_B$  and  $H_C = 300$  Oe for the 7.5 nm film are observed. The temperature dependence of  $M$  measured with  $H$

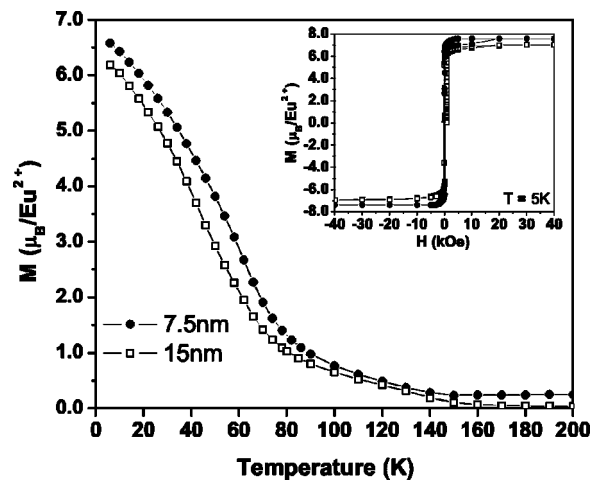


FIG. 2. Magnetization vs temperature taken with  $H = 800$  Oe for 15 and 7.5 nm EuO films, showing a  $T_C$  close to that of bulk EuO, 69 K. Inset:  $M(H)$  at 5 K showing a magnetic moment closely matching bulk moment,  $7.45\mu_B$ .  $M$  is given in  $\mu_B$  per Eu<sup>2+</sup> ion.

$= 800$  Oe for these two films is shown in Fig. 2. The observed  $T_C$  closely matches the  $T_C$  of bulk EuO, 69 K. The 7.5 nm film has a slightly better moment and  $M_r$  in comparison to the 15 nm film, even though both were made with the same deposition rate and oxygen flow. This may be because the 7.5 nm film was made in the same run after the 15 nm film, and thus had a better background vacuum due to the getter action of deposited Eu on the chamber walls.

Even though XRD, optical, and SQUID characterization show that high quality EuO film was successfully grown, these techniques are not as useful in determining if a few monolayers of EuO as a tunnel barrier are successfully prepared by the same method. However, due to its sensitivity to barrier and interface quality, spin-polarized tunneling measurement is an excellent method to determine the quality of the ultrathin EuO and detect the spin-filter effect.<sup>11</sup> Tunnel junctions were cooled to 0.45 K in a <sup>3</sup>He cryostat and current ( $I$ )-voltage ( $V$ ) characteristics were measured. The tunneling dynamic conductance ( $dI/dV$ ) versus bias voltage is shown in Fig. 3(a) for a 4.5 nm Al/4.5 nm EuO/25 nm Ag junction. The superconducting transition temperature of the 4.5 nm Al was 2.23 K. Conductance was measured prior to applying a magnetic field. The superconducting energy gap of Al centered at  $V = 0$  is clearly observed. Then a field  $H_{\text{appl}} = 0.27$  T was applied in the film plane. A large Zeeman splitting of the Al quasiparticle density of states is observed. The magnitude of this splitting ( $= 2\mu_B H_0$ ) corresponds to a total effective field of  $H_0 = 3.5$  T, even though  $H_{\text{appl}} = 0.27$  T. The Zeeman splitting is enhanced by the internal exchange field  $H^* = H_0 - H_{\text{appl}} = 3.2$  T, produced by the ferromagnetically ordered Eu<sup>2+</sup> ions acting on the conduction electrons in the Al by a proximity interaction at the EuO/Al interface.<sup>26,27</sup> This enhanced Zeeman splitting has been seen for all EuO junctions and is a clear indication that ferromagnetic EuO is present in the barrier. More importantly, a polarization of 9% is determined from the conductance curve, as the asymmetry shows that the tunnel current is spin polarized.<sup>11,15</sup> As the electrodes are not FMs (and thus not a

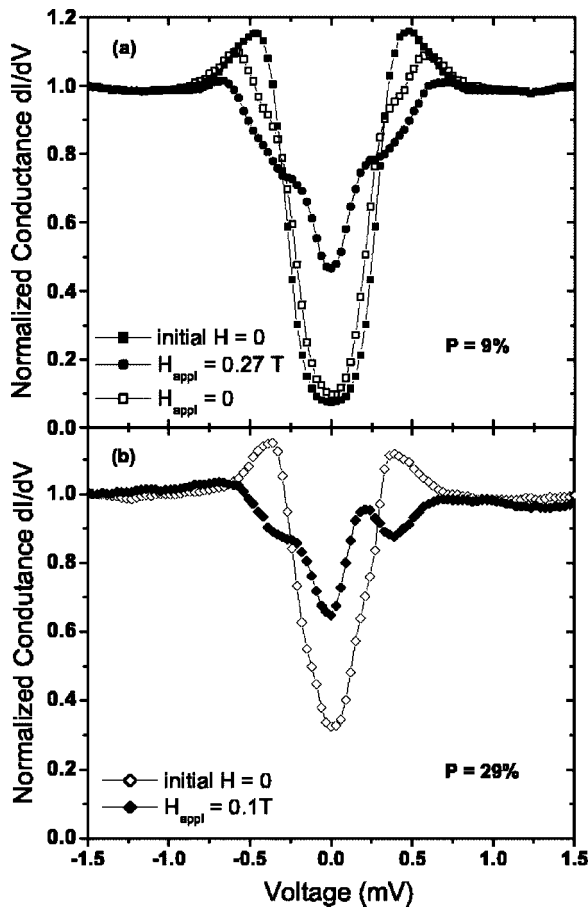


FIG. 3. Tunnel conductance  $dI/dV$  as a function of applied voltage across junctions with an EuO tunnel barrier, measured at 0.45 K. (a)  $dI/dV$  for 4.5 nm Al/4.5 nm EuO/25 nm Ag junction. (b)  $dI/dV$  for 4.2 nm Al/1.4 nm EuO/5 nm Y/10 nm Al junction.

source for polarized spins), the measured polarization demonstrates that spin filtering is occurring in the EuO barrier. After reducing the applied field back to zero [ $H_{\text{appl}}=0$  in Fig. 3(a)], the conductance curve continues to display Zeeman splitting. Furthermore, asymmetry of this curve shows that polarization remains even at zero field. This is due to the remanent magnetization state of EuO. Although higher  $P$  is to be expected, this is a demonstration of spin filtering in an ultrathin EuO barrier.

A larger  $P$  is obtained when an yttrium electrode is used, as shown in Fig. 3(b) for a 4.2 nm Al/1.4 nm EuO/5 nm Y/10 nm Al junction. Conductance was measured initially in zero field and then at  $H_{\text{appl}}=0.1$  T. A polarization of 29% is determined from the spin-split, asymmetric conductance curve at  $H_{\text{appl}}=0.1$  T. The enhanced Zeeman splitting corresponds to a total effective field of  $H_0=3.9$  T. Thus, there is an even larger internal exchange field ( $H^*=3.8$  T) seen by the quasiparticles of superconducting Al from the EuO bar-

rier of this sample. The higher  $P$  results from more efficient spin filtering in this junction with a Y top electrode, compared to the junction with a Ag top electrode. This is attributed to the better quality of EuO (having less  $\text{Eu}_2\text{O}_3$  present), which can be expected since Y readily oxidizes to form  $\text{Y}_2\text{O}_3$  ( $\Delta H_f=-1760$  kJ/mol)<sup>22</sup> and is likely to be reducing the  $\text{Eu}_2\text{O}_3$  phase at the interface, leading to a purer EuO phase.

Zeeman splitting induced by the internal exchange field is observed in the final  $H_{\text{appl}}=0$  curve [see Fig. 3(a)] but not in the initial zero field curve. This can be explained as due to the randomly magnetized multidomain structure of the EuO film. Initially, at zero field,  $L \ll \xi$  where  $L$  is the domain size and  $\xi$  is the superconducting coherence length.<sup>16</sup> The domains are randomly oriented prior to applying the field, and the Al quasiparticles over an area  $\xi^2$  see a net exchange field of zero. In the saturated condition (nearly single domain state), a large exchange field results, exhibiting significantly enhanced Zeeman splitting. In the remanent magnetization state ( $H=0$ ),  $L \gg \xi$  and splitting is still observed. However, for the second set of samples, careful observation shows Zeeman splitting and conductance asymmetry (polarization) in the pristine state even before a field was applied [initial  $H=0$  curve in Fig. 3(b)]. Since a larger portion of the barrier is EuO, with less  $\text{Eu}_2\text{O}_3$  phase present as described earlier, the domains are larger; giving rise to a net average exchange field that induces Zeeman splitting in the Al. Data shown in Fig. 3(b) are consistent with the better quality of EuO formed and shows the trend to achieve 100% spin filtering. Notably, while  $P$  is a direct consequence of the spin-filter effect, enhanced Zeeman splitting is a separate consequence of the ferromagnetic ordering in the EuO.<sup>16,27</sup>

From the current-voltage characteristics at 0.45 K (in the magnetized state of EuO), an average barrier height  $\Phi=0.2$  eV and a barrier thickness  $S=5$  nm were obtained.<sup>18</sup>  $S$  is consistent with the evaporated EuO thickness of 4.5 nm, whereas  $\Phi$  is significantly low, indicating states in the energy gap region of EuO due to nonstoichiometry.<sup>28,29</sup> However, it is encouraging to see sizable polarization despite the defect states in the barrier.

In summary, ultrathin films of EuO were successfully prepared by reactive evaporation and show structure, optical, and magnetic properties matching that of bulk EuO. Spin-polarized tunneling measurement through an ultrathin EuO film, used as a tunnel barrier between nonferromagnetic electrodes, showed significant polarization due to spin filtering of the tunnel current through the exchange-split barrier heights of EuO. The EuO spin filter is a promising tunnel barrier for efficient spin injection into semiconductors.

This work is supported by NSF funding and T.S.S. is partially supported by NSF.

\*Also at: Department of Materials Science and Engineering, MIT.

- <sup>1</sup>*Semiconductor Spintronics and Quantum Computation*, edited by D. D. Awschalom, D. Loss, and N. Samarth (Springer, New York, 2002).
- <sup>2</sup>M. Oestreich, M. Bender, J. Hübner, D. Hägele, W. W. Rühle, Th. Hartmann, P. J. Klar, W. Heimbrodt, M. Lampalzer, K. Volz, and W. Stolz, *Semicond. Sci. Technol.* **17**, 285 (2002).
- <sup>3</sup>R. Fiederling, M. Keim, G. Reuscher, W. Ossau, G. Schmidt, A. Waag, and L. W. Molenkamp, *Nature (London)* **402**, 787 (1999).
- <sup>4</sup>Y. Ohno, D. K. Young, B. Beschoten, F. Matsukura, H. Ohno, and D. D. Awschalom, *Nature (London)* **402**, 790 (1999).
- <sup>5</sup>G. Schmidt, D. Ferrand, L. W. Molenkamp, A. T. Filip, and B. J. van Wees, *Phys. Rev. B* **62**, R4790 (2000).
- <sup>6</sup>B. T. Jonker, Y. D. Park, B. R. Bennett, H. D. Cheong, G. Ki-oseoglou, and A. Petrou, *Phys. Rev. B* **62**, 8180 (2000).
- <sup>7</sup>H. J. Zhu, M. Ramsteiner, H. Kostial, M. Wassermeier, H. P. Schönherr, and K. H. Ploog, *Phys. Rev. Lett.* **87**, 016601 (2001).
- <sup>8</sup>V. F. Motsnyi, J. De Boeck, J. Das, W. Van Roy, G. Borghs, E. Goovaerts, and V. I. Safarov, *Appl. Phys. Lett.* **81**, 265 (2002).
- <sup>9</sup>T. Manago and H. Akinaga, *Appl. Phys. Lett.* **81**, 694 (2002).
- <sup>10</sup>E. I. Rashba, *Phys. Rev. B* **62**, R16 267 (2000).
- <sup>11</sup>R. Meservey and P. M. Tedrow, *Phys. Rep.* **238**, 173 (1994).
- <sup>12</sup>J. Schoenes and P. Wachter, *Phys. Rev. B* **9**, 3097 (1974).
- <sup>13</sup>P. Wachter, in *Handbook on the Physics and Chemistry of Rare Earths*, edited by K. A. Schneider and L. Eyring (North-Holland Publishing Co., New York, 1979), Vol. 2, p. 507.
- <sup>14</sup>P. G. Steeneken, L. H. Tjeng, I. Elfimov, G. A. Sawatzky, G. Ghiringhelli, N. B. Brookes, and D. J. Huang, *Phys. Rev. Lett.* **88**, 047201 (2002).
- <sup>15</sup>J. S. Moodera, X. Hao, G. A. Gibson, and R. Meservey, *Phys. Rev. Lett.* **61**, 637 (1988).
- <sup>16</sup>X. Hao, J. S. Moodera, and R. Meservey, *Phys. Rev. B* **42**, 8235 (1990).
- <sup>17</sup>J. S. Moodera, R. Meservey, and X. Hao, *Phys. Rev. Lett.* **70**, 853 (1993).
- <sup>18</sup>W. F. Brinkman, R. C. Dynes, and J. M. Rowell, *J. Appl. Phys.* **41**, 1915 (1970).
- <sup>19</sup>M. W. Shafer and T. R. McGuire, *J. Appl. Phys.* **39**, 588 (1968).
- <sup>20</sup>S. Von Molnar and M. W. Shafer, *J. Appl. Phys.* **41**, 1093 (1970).
- <sup>21</sup>T. Matsumoto, K. Yamaguchi, K. Yamada, and K. Kawaguchi, *Mater. Sci. Forum* **373-376**, 369 (2001).
- <sup>22</sup>*The Oxide Handbook*, 2nd ed., edited by G. V. Samsonov (IFI/Plenum, New York, 1982).
- <sup>23</sup>Powder reference from Jade software for XRD analysis (Materials Data, Incorporated).
- <sup>24</sup>J. Lettieri, V. Vaithyanathan, S. K. Eah, J. Stephens, V. Sih, D. D. Awschalom, J. Levy, and D. G. Schlom, *Appl. Phys. Lett.* **83**, 975 (2003).
- <sup>25</sup>G. Güntherodt, J. Schoenes, and P. Wachter, *J. Appl. Phys.* **41**, 1083 (1970).
- <sup>26</sup>P. M. Tedrow, J. E. Tkaczyk, and A. Kumar, *Phys. Rev. Lett.* **56**, 1746 (1986).
- <sup>27</sup>X. Hao, J. S. Moodera, and R. Meservey, *Phys. Rev. Lett.* **67**, 1342 (1991).
- <sup>28</sup>R. Meservey, P. M. Tedrow, and J. S. Brooks, *J. Appl. Phys.* **53**, 1563 (1982).
- <sup>29</sup>G. A. Gibson and R. Meservey, *J. Appl. Phys.* **58**, 1584 (1985).